

## POSSIBILITY OF ESPI VISUALIZATION OF SOUND PRESSURE FIELDS

Zdeněk Otčenášek, Pavel Dlask

Sound Studio of Music Faculty  
Academy of Performing Arts in Prague  
otcenasek@hamu.cz

### ABSTRACT

Electronic speckle pattern interferometers (ESPI) are prominent helping tools for non contact observations of movements of an object surface. Their functionality is based on speckles, which are products of the interference effect between both the laser beams scattered from separate unevenness of the object rough surface and the reference beam originated from the same laser source. This method is applicable on rough surfaces of solids. In the case of acoustic fields the air particles don't give speckle patterns. Also in this case ESPI visualization can be used, but based on a principle of changes in the air refractive index when air pressure is changed. The aim of this contribution is to explain basic know-how and possibilities of ESPI (especially double pulse TV ESPI method) visualizations of a sound pressure distribution in a defined space. The practical output is focused on applications on wind musical instruments (presented is an example of sound pressure distribution inside and outside of an organ pipe in the process of normal excitation).

### 1. INTRODUCTION

Electronic speckle pattern interferometers (ESPI) allow non contact observations of movements of an object surface (full-field manner). The double pulse TV ESPI method visualizes relative displacements. The relativity of such movement observations rises from the matching of two speckle images: reference state and recording state (the principle of ESPI see Figure 1). Both images are recorded by one CCD camera, when the object is illuminated with a sequence of two flashes of a pulse laser. On both images the speckles are visible. The speckles are products of the interference effect between both the laser beam scattered from separate unevenness of the object rough surface and the reference beam originated from the same laser source. In accordance with the value of the phase shift between both beams, a darker (both beams are with opposite phase) or a brighter (beams are in coincidence) spot is created on the pixel of the camera. This spots are called speckles.

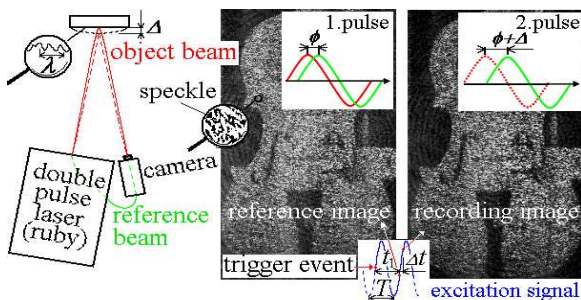


Figure 1: The principle of a reference and recording speckle image creation. The object beam passes through the camera after reflecting from the surface points; the reference beam is lead to the camera through an optical fiber (used example is from a violin surface observation).

The correlation of obtained speckles and the subtraction of its hue in both the reference and recording image give a speckle intensity image with a pattern of fringes (contour lines in positions with equal extent of deflection due to deformations or movements, Figure 2). But the speckle intensity image itself does not inform about directions of displacements and thus about relations between fringes.

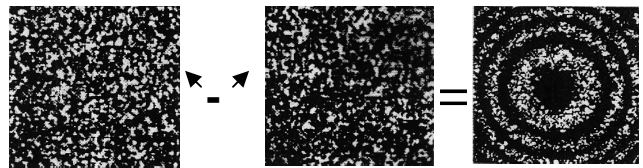


Figure 2: Intensity pattern (right) created from reference (left) and recording (midst) speckles. The fringes (right) are contours of the same intensity (gray grades) and denote surface points with identical values of displacement per time between both laser pulses.

Therefore, the pixels intensity values  $I$  from this obtained intensity image are further used in a system of equations for the calculations of laser beam phase shifts ( $\Delta\phi$  due to a surface point displacement per time between both laser pulses). Here a trick is used. For this system of equations to be solved, the phase difference between neighboring reference beams, which illuminate separate pixels in one row of the CCD camera sensor, is  $+2/3\pi$ . This phase increases progressively through all pixels of a row. Then the values of a phase shift of a pixel (at image coordinates  $x_n, y$ ) can be computed from intensities of this pixel and intensities of both neighboring pixels ( $x_{n-1}, y$  and  $x_{n+1}, y$ ) in the same row:

$$\Delta\phi(x_n, y) = \arctan \left[ \sqrt{3} \frac{I(x_{n-1}, y) - I(x_{n+1}, y)}{2I(x_n, y) - I(x_{n-1}, y) - I(x_{n+1}, y)} \right], (1)$$

Obtained values of pixel phase shifts are then elements of a resulting phase image (Figure 3 Left). This image already includes information about directions of the surface point displacements.

The phase image could be further mapped in a suitable color scale. Then the points with negative (e.g. in Figure 3 Right: blue, green) and positive (here: yellow, red) directions of displacement are well distinguishable through different colors.

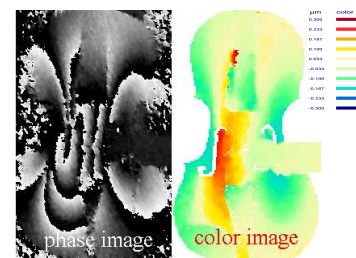


Figure 3: Movements of all surface points simultaneously observed in one selected time relatively to a used trigger event.

Since in the double pulse ESPI method both the time delay  $t_1$  of the first flash after a defined trigger event (e.g. the zero crossing of a movement excitation, see Figure 4) and also the laser pulse separation time  $\Delta t$  are adjustable, repeating the double flashing after readjusting the  $t_1$  gives a possibility to follow the deformation changes in time.

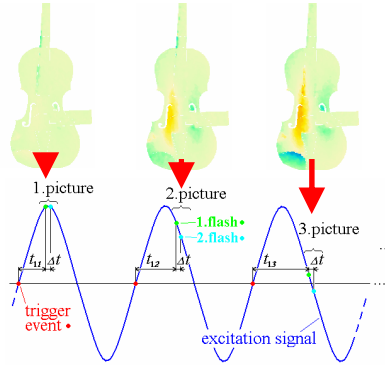


Figure 4: Adjusting the laser double pulses relatively to the triggered event and following the surface movements in time (capturing different stages of a displacement).

## 2. GASEOUS ENVIRONMENT

These explicit ESPI principles are applicable on rough reflecting surfaces, usually of solids. If an acoustic field (certain sound pressure spreading in a 3D space) has to be visualized, then we must use a suitable finesse, because the air particles don't give speckle patterns. In those cases it is possible to utilize the changes of the air refractive index ( $n$ ) when air density ( $\rho$ ), pressure ( $p$ ) or temperature ( $T$ ) is changed (it changes the velocity of laser light propagation). Their relationship solves the **Gladston – Dale** relation:

$$n = \frac{c_0}{v} = 1 + 2,2563 \cdot 10^{-4} \cdot \rho = 1 + 7,8607 \cdot 10^{-7} \cdot \frac{p}{T} \quad (2)$$

Total air pressure in a space point  $X(x, y, z)$  in an acoustic field has an in time invariant part ( $p_{normal}=101325\text{Pa}/20^\circ\text{C}$ ) and a variable part due to sound source (sound pressure  $\Delta p$ ):

$$p_X(t, xyz_X) = p_{air,normal} + \Delta p_X(t, xyz_X) \quad (3)$$

The time flow of laser light intensity in air in normal conditions ( $\Delta p = 0$ ) can be described by the solution of a wave propagation equation (without losses):

$$I(t, d) \approx I_0 \cdot e^{i\omega_{air,normal} \left( t - \frac{d \cdot n_{air,normal}}{c_0} \right)} \quad (4)$$

where:  $\omega_{air,normal}$  is light circular frequency,  $t$  is time,  $c_0$  is lights velocity in vacuum,  $d$  is the distance on beam from a source (see Figure 5 Left),  $n_{air,normal}$  is air refractive index joined with lights velocity in air  $v$  through the relation  $n_{air,normal} = c_0 / v_{air,normal}$ .

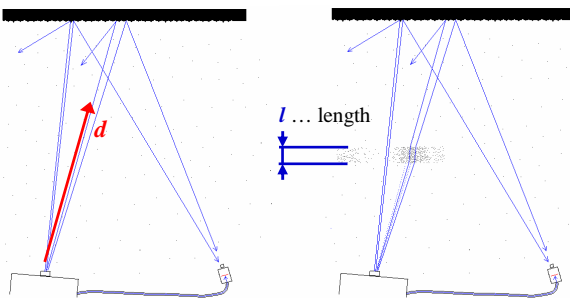


Figure 5: Laser beams reflections and scatterings. Left: Beam propagation through air. Right: Beam passing through inserted gaseous environment with features different to air.

A gaseous environment (whose features differ from the normal air) inserted into the lights path (Figure 5 Right, Figure 6) changes the lights velocity (and the value of the refraction index; such environment can also be the air, whose pressure differs from  $p_{normal}$ ). Due to this different velocity ( $v_{environm.} \neq v_{air}$ ) the propagated light goes through this environment (length  $l$  in the path of light) in a different time in comparison to normal air ( $t_{air+environm.} \neq t_{air}$ ). If the lights incidence at the environment boundary has a perpendicular angle (Figure 6 Left), this time difference is:

$$\Delta t = t_{air} - t_{air+environm.} = \frac{l \cdot (n_{air} - n_{environm.})}{c_0} \quad (5)$$

If the incidence is non perpendicular (Figure 6 Right), light beam diffractions occur. However, since the Fermat's principle of 'shortest time' is valid, thus, all sketched light paths (without and with diffractions) have the same time difference. Then it is possible to calculate with the same length  $l$  of passing through the medium as if it would be on a straight line from the source on the path without diffraction (red arrow in Figure 6 Right).

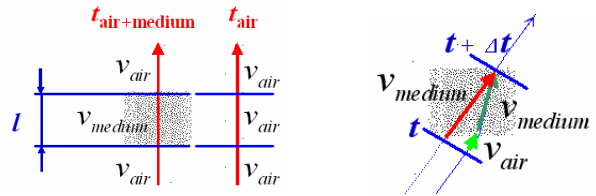


Figure 6 Left: perpendicular angle of light beam incidence at an environment (in Figure 6 cold medium) boundary. Right: non perpendicular incidence; the straight-line path of light beam (here marked with a red arrow) has the same passing time  $\Delta t$  as has the path with diffraction (both green arrows together); the phase of the light after passing through both these trajectories (red and green) is identical.

This explicit time difference  $\Delta t$  has to be subtracted in the solution of the wave propagation:

$$\begin{aligned} I(t, d) &\approx I_0 \cdot e^{i\omega_{air,normal} \left( t - \frac{d \cdot n_{air,normal}}{c_0} \right)} = \\ &= I_0 \cdot e^{i\omega_{air,normal} \left( t - \frac{l \cdot (n_{air,normal} - n_{environm.})}{c_0} - \frac{d \cdot n_{air,normal}}{c_0} \right)} = \\ &= e^{-i\omega_{air,normal} \cdot \frac{l \cdot (n_{air,normal} - n_{environm.})}{c_0}} \cdot \underbrace{I_0 \cdot e^{i\omega_{air,normal} \left( t - \frac{d \cdot n_{air,normal}}{c_0} \right)}}_{\text{time flow of lights intensity in air without inserted environment}} \quad (6) \end{aligned}$$

From this result arises, that the changes of the refraction index change the phase  $\Delta\theta$  of the recorded light beam. If we illuminate the non moving surface in the background through the part of the air (or through other inserted gaseous environments), where the different features are, this surface at the speckle pictures seems as if it is relocated.

The example in Figure 7 illustrates the similarity of a displacement of a surface in the background (Left) with a situation in which an acoustic field is inserted (Right: the beam path with a diffraction goes through an area of higher pressure symbolized with more black dots; also the beam path in an area, where sound pressure has null value and no additional diffraction occurs, is demonstrated). Such presented sketch of a sound pressure distribution can arise e.g. in a transparent box and can originate e.g. through a standing wave excitation.

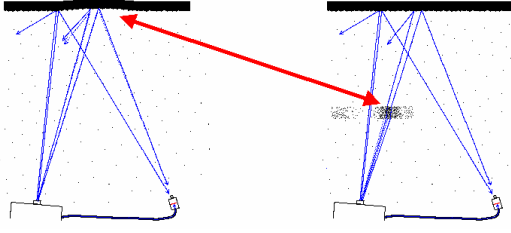


Figure 7: Due to light beams phase changes, the non moving surface in the background, illuminated through an environment with diverse features, seems on the camera speckle pictures as if it is displaced.

The air in normal conditions has its refraction index very low:  $n_{airnormal} = 1.0002718029$  ( $\lambda = 632.8 \text{ nm} / p_{normal}$ ). If the sound pressure level is 100 dB, the air pressure alters from the normal value  $p(t, xyz_x) = 101325 \text{ Pa}$  to values between peak values (normal + acoustic)  $p(t, xyz_x) = -101323$  and  $+101327 \text{ Pa}$ . Then the refraction index varies up to the peak value (substituted in the relation 2; taken only + value):

$$n_{airnormal+acoustic} = 1 + 7,8607 \cdot 10^{-7} \cdot \frac{101327}{293} = 1,0002718434$$

and shift of phase ( $\Delta\theta$  in the relation 6 after substitution) is:

$$\Delta\theta \cong \frac{360.3 \cdot 10^5}{6,328 \cdot 10^{-7}} \cdot \frac{0,1(1,0002718029 - 1,000271843)}{3 \cdot 10^5} = +2,3^\circ$$

Even though the sound pressure level of 100dB is great in a usual acoustic environment, it is still not sufficient for ESPI visualization. Such a small phase shift ( $1/78\pi$ ) is not recognizable with this technique. Generally, a good differentiation of very small phase shifts with double pulse TV holography method is influenced: 1) by the adjustment of laser illumination and 2) by relative displacement of a surface in the background. For this type of sound pressure visualization the self vibrations of both the background surface and also the ESPI laser head (and camera) are not negligible, because we must use a long interval between the first reference pulse (which illuminates the background through air in its standing stage) and second recording pulse (which illuminates the background in synchrony with a temporal course of an observed air feature, here in synchrony with course of sound pressure). These self vibrations are excited mainly by the motion of the building (can be evoked also through an acoustic way). Even if these vibrations are minimized, they always bring a measurement noise (usually comparable with phase shifts up to  $1/10\pi$ ).

The simplest solution to this sensitivity problem is to increase the refraction index (and thus its changes) in the inserted environment or to have a substantially greater distance  $l$ . Since  $\text{CO}_2$  has its refraction index relatively sufficient ( $n_{\text{CO}_2 \text{ normal}} = 1,0004174 / 20^\circ\text{C}$ ,  $p_{normal}$ ) and air contains it, it is possible to increase air refraction index through mixing this gas with normal air (the increase of  $\text{CO}_2$  concentration). The  $\text{CO}_2$  concentration would be chosen in correlation to distance  $l$  of an inserted environment and to the peak values of sound pressure. A suitable shift of phase  $\theta$  would be approximately  $\pi$  and more. In the case of wind musical instruments, when their sound is excited naturally by an air flow, the mixing of  $\text{CO}_2$  with air can be done similarly as in a cars carburetor.

### 3. MEASUREMENT EXAMPLE

Figure 8 presents an example of a use of a mixture of 80% volume unit of normal air with 20% volume unit of pure  $\text{CO}_2$  ( $20^\circ\text{C}$ ,  $p_{normal}$ ) for visualization of sound pressure inside

and outside of an organ pipe in the process of normal excitation (both side walls of this pipe were from glass).

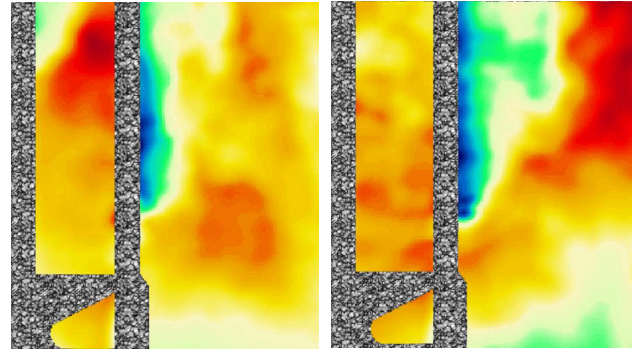


Figure 8: Distributions of sound pressure inside and outside of an organ pipe in the process of normal excitation.

The images (Figure 8) show two different sound excitation stages that are captured in synchrony with the sound pressure recorded by a microphone. Red (and yellow, see scale in Figure 9) colors in images visualize areas in these environments with positive laser light phase shift. This is caused by the positive values of sound pressure in those areas, which cause lower values of velocities of laser beams passing this way and therefore higher values of refraction index in comparison to normal air. The blue (and green) colors visualize opposite values (the relations  $p$ ,  $n$ ,  $v$  and theirs mapping to a color are:

$$p_{airnormal+SP} - p_{airnormal} \rightarrow n_{environm.} - n_{air} \rightarrow v_{air} - v_{environm.} > 0 \rightarrow \text{red/yellow}$$

$$p_{airnormal+SP} - p_{airnormal} \rightarrow n_{environm.} - n_{air} \rightarrow v_{air} - v_{environm.} < 0 \rightarrow \text{blue/green}$$

Such relations between ESPI images color scale and positive or negative difference of environment features can be well demonstrated in an image example (Figure 9), in which a  $\text{CO}_2$  environment or only a hot air environment is used (Figure 9 Left:  $\text{CO}_2$  jet decreases lights velocity; Right: hot air jet increases lights velocity; both environments were produced as a jet in air).

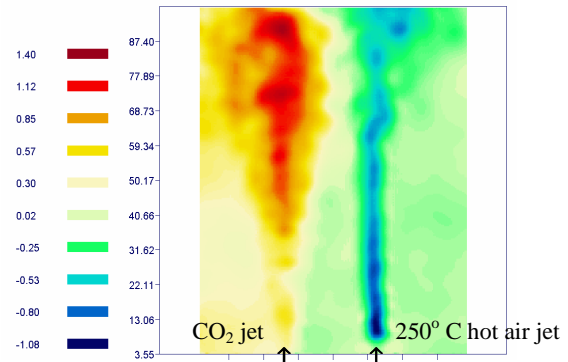


Figure 9: Positive phase shift of laser light in a  $\text{CO}_2$  jet (red and yellow colors) and negative phase shift in a hot air jet (blue and green). Both jets go from its sources  $\uparrow$  bottom-up.

### 4. CONCLUSIONS

The presented method of sound pressure visualization appears to be an applicable way to study such problems, where other methods are often complicated or do not exist. In this paper the practical outputs are focused on applications on wind musical instruments, especially on organ pipes, but this can be extended on other spheres of interest, based on air density, pressure or temperature changes. Of course, even if the use of this method is simple, in cases where the studied gaseous environments are inside boxes, a complication can arise, because these boxes must be constructed to be transparent for laser light.